Distal Radius in Adolescent Girls with Anorexia Nervosa: Trabecular Structure Analysis with High-Resolution Flat-Panel Volume CT[1]

Miriam A. Bredella, MD
Madhusmita Misra, MD, MPH
Karen K. Miller, MD
Ijad Madisch, MD
Ammar Sarwar, MD
Arnold Cheung, MD
Anne Klibanski, MD
Rajiv Gupta, MD, PhD

Purpose: To examine trabecular microarchitecture with high-resolution flat-panel volume computed tomography (CT) and bone mineral density (BMD) with dual-energy x-ray absorptiometry (DXA) in adolescent girls with anorexia nervosa (AN) and to compare these results with those in normal-weight control subjects.

Materials and Methods: The study was approved by the institutional review board and complied with HIPAA guidelines. Informed consent was obtained. Twenty adolescent girls, 10 with mild AN (mean age, 15.9 years; range, 13–18 years) and 10 age- and sex-matched normal-weight control subjects (mean age, 15.9 years; range, 12–18 years) underwent flat-panel volume CT of distal radius to determine apparent trabecular bone volume fraction (BV/TV), apparent trabecular number (TbN), apparent trabecular thickness (TbTh), and apparent trabecular separation (TbSp). All subjects underwent DXA of spine, hip, and whole body to determine BMD and body composition. The means and standard deviations (SDs) of structure parameters were calculated for AN and control groups. Groups were compared (Student *t* test). Linear regression analysis was performed.

Results: AN subjects compared with control subjects, respectively, showed significantly lower mean values for BV/TV (0.37% ± 0.05 [SD] vs 0.46% ± 0.03, $P = .0002$) and TbTh (0.31 mm ± 0.03 vs 0.39 mm ± 0.03, $P < .0001$) and higher mean values for TbSp (0.54 mm ± 0.13 vs 0.44 mm ± 0.04, $P = .02$). TbN was lower in AN subjects than in control subjects, but the difference was not significant (1.17 mm^{-3} ± 0.15 vs 1.22 mm^{-3} ± 0.07, $P = .43$). There was no significant difference in BMD between AN and control subjects. BMD parameters showed positive correlation with BV/TV and TbTh in the control group ($r = 0.55–0.84$, $P = .05–.01$) but not in AN patients.

Conclusion: Flat-panel volume CT is effective in evaluation of trabecular structure in adolescent girls with AN and demonstrates that bone structure is abnormal in these patients compared with that in normal-weight control subjects despite normal BMD.

Supplemental material: *http://radiology.rsnajnls.org/cgi/content/full/249/3/938/DC1*

[1] From the Department of Radiology (M.A.B., I.M., A.S., A.C., R.G.), and Neuroendocrine Unit, Department of Medicine (M.M., K.K.M., A.K.), Massachusetts General Hospital, 55 Fruit St, Yawkey 6E, Boston, MA 02114; and Pediatric Endocrine Unit, Massachusetts General Hospital for Children, Boston, Mass (M.M.). Received January 26, 2008; revision requested March 19; revision received April 3; accepted April 28; final version accepted May 13. Supported by National Institutes of Health grants ROI DK062249, K23 RR018851, and MO1 RR01066. **Address correspondence to** M.A.B. (e-mail: *mbredella@partners.org*).

Low bone mineral density (BMD) is a serious complication of anorexia nervosa (AN) in adults and adolescents (1,2). Decreased bone mass occurs in multiple skeletal sites and is associated with a sevenfold increased fracture risk that may persist despite recovery (3,4). The onset of AN during the adolescent years is of particular concern because this is a crucial time for bone mass accrual toward achievement of peak bone mass. Deficits in the normal rate of bone mass accrual during this period can result in low peak bone mass and an increased risk of fractures in adult life (2,5). Dual-energy x-ray absorptiometry (DXA) is commonly used for the assessment of BMD; however, it is highly influenced by body size (6), which provides a diagnostic challenge in children with AN, because prolonged undernutrition can potentially affect statural growth, which in turn leads to smaller bones. Strength is determined not only by BMD but also bone structure. Quantitative ultrasonography (US) has been used in patients with AN (7,8). However, quantitative US generates global measures of bone density and cannot provide information on bone architecture. Quantitative computed tomography (CT) allows direct measurement of "true" volumetric BMD, which is advantageous in children because of the growth-related variations in bone size (9); however, quantitative CT does not provide information on bone architecture.

Researchers in several studies have suggested that alterations in bone architecture could explain bone fragility and fracture risk independent of BMD (10–16) and that assessment of trabecular bone microarchitecture may improve the prediction of fracture risk and the capability to monitor the response to therapeutic intervention (17,18). Evaluating bone mass with only BMD by using DXA, quantitative US, or quantitative CT, therefore, may be insufficient to fully assess biomechanical strength of trabecular bone or fracture risk (19,20).

The literature about trabecular microarchitectural changes in AN is sparse (21–23), and, to our knowledge, no prior study has been performed about trabecular microarchitecture in adolescents with AN. In the present study, we introduce the use of high-resolution flat-panel volume CT for the evaluation of trabecular bone structure in adolescent girls with AN and compare the results with those in normal-weight control subjects.

Flat-panel volume CT is an imaging modality that combines the advances in CT with digital flat-panel–detector technology and is capable of high-resolution ($150 \times 150 \times 150$-μm) in vivo imaging (24–26). There are other high-resolution CT scanners, such as the high-resolution peripheral quantitative CT scanner, with a spatial resolution of approximately 80 μm (16,27), and the micro-CT scanner, used for in vitro or small-animal imaging, with a spatial resolution of approximately 10–20 μm (17,27). In contrast, the resolution of a conventional multidetector CT scanner is approximately 500×500 μm in plane and 500–1000 μm along the z-axis (28).

Given the importance of the accrual of peak bone mass during adolescence, the purpose of our study was to prospectively examine trabecular microarchitecture by using flat-panel volume CT and to evaluate BMD by using DXA in adolescent girls with AN and to compare these results with those in age- and sex-matched normal-weight control subjects. We hypothesized that parameters of bone microarchitecture would be adversely affected in AN patients regardless of BMD findings, as assessed by using DXA.

Advances in Knowledge

- Flat-panel volume CT allows evaluation of trabecular structure in adolescents with anorexia nervosa (AN).
- Bone structure is abnormal in adolescents with AN compared with normal-weight control subjects despite normal bone mineral density (BMD).
- Trabecular structure parameters correlate with BMD in normal-weight control subjects but not in patients with AN.

Implication for Patient Care

- Flat-panel volume CT can be used as a noninvasive technique for evaluation of trabecular structure in adolescents with AN.

Materials and Methods

Patients

The study was approved by our institutional review board and complied with Health Insurance Portability and Accountability Act guidelines. Written informed consent was obtained from all subjects and their parents after the nature of the procedure had been fully explained.

Between May and December of 2007, we examined a total of 20 girls aged 12–18 years, with a mean age of 15.9 years ± 1.8 standard deviation (SD) and an age range of 12.6–18.6 years. These subjects included 10 adolescent girls with AN (mean age, 15.9 years ± 1.6; range 13.8–18.2 years) and 10 normal-weight age- and sex-

Published online
10.1148/radiol.2492080173

Radiology 2008; 249:938–946

Abbreviations:
AN = anorexia nervosa
BMD = bone mineral density
BMI = body mass index
BV/TV = apparent trabecular bone volume fraction
DXA = dual-energy x-ray absorptiometry
SD = standard deviation
TbN = apparent trabecular number
TbSp = apparent trabecular separation
TbTh = apparent trabecular thickness

Author contributions:
Guarantors of integrity of entire study, M.A.B., R.G.; study concepts/study design or data acquisition or data analysis/interpretation, all authors; manuscript drafting or manuscript revision for important intellectual content, all authors; manuscript final version approval, all authors; literature research, M.A.B., M.M., K.K.M., I.M., A.K.; clinical studies, all authors; experimental studies, M.A.B., M.M., R.G.; statistical analysis, M.A.B., M.M., A.C.; and manuscript editing, M.A.B., M.M., K.K.M., A.S., A.C., A.K., R.G.

Authors stated no financial relationship to disclose.

matched healthy control subjects (mean age, 15.9 years ± 2.1; range, 12.6–18.2 years). The diagnosis of AN was confirmed by the study psychiatrist on the basis of *Diagnostic and Statistical Manual of Mental Disorders*, fourth edition, criteria. These criteria include *(a)* refusal to maintain body weight at or above a minimally normal weight for age and height; *(b)* intense fear of gaining weight or becoming fat, even though underweight; *(c)* disturbance in the way in which one's body weight or shape is experienced, undue influence of body weight or shape on self-evaluation, or denial of the seriousness of the current low body weight; and *(d)* in postmenarcheal female subjects, amenorrhea (ie, the absence of at least three consecutive menstrual cycles). AN subjects had mild illness in that, although all met the criteria for diagnosis, they were more than 80% ideal body weight for age. The age- and sex-matched healthy control subjects had a body mass index (BMI) that was between the 5th and 95th percentiles, and all had more than 90% ideal body weight for age. Disease duration ranged from 0.5 to 22 months (mean, 13.8 months ± 11.8). AN subjects were referred to the study by eating disorder providers in the area, and healthy control subjects were recruited through mass mailings to pediatricians and adolescent medicine physicians and through advertisements within our health care system. AN subjects and healthy control subjects were examined during one study visit at our General Clinical Research Center. BMI was calculated by using the formula BMI = W/H, where W is weight in kilograms and H is height in square meters. A complete history was recorded and a physical examination was performed. All subjects underwent anteroposterior radiography of the left hand for determination of skeletal age, according to the standards determined by Greulich and Pyle (29).

Exclusion criteria for the two groups included pregnancy, presence of chronic disease (other than AN) known to affect bone density, and abnormal thyroid-stimulating hormone level (reference range, 0.4–5.0 μU/mL) or a high follicle-stimulating hormone level (<10 U/L). No control subject had a history of an eating disorder or had an eating disorder at the time of the study. Two subjects in the AN group and none of the subjects in the control group were receiving oral contraceptives. Four subjects in the AN and three subjects in the control group were receiving calcium supplements, and eight subjects in the AN and two subjects in the control group received multivitamins. None of the subjects smoked cigarettes at time of the study.

High-Resolution Flat-Panel Volume CT

To determine differences in bone microarchitecture between adolescent girls with AN and healthy control subjects, CT of the distal radius was performed by using flat-panel volume CT.

The flat-panel volume CT prototype (Siemens, Forchheim, Germany) consists of a CT gantry with a bore diameter of 40 cm integrated with a modified x-ray tube and a two-dimensional digital flat-panel detector system. The digital flat-panel detector employs a thin film of scintillator crystals, grown on a matrix of photograph detectors fabricated on an amorphous silicon wafer, to convert incident x-ray energy to light. There are 2048 × 1536 elements in the matrix of photograph detectors, each measuring 194 × 194 μm^2. A total of 580 projection images were acquired over a 360° angular span, with tube voltage ranging from 80 to 120 kV and tube current ranging from 10 to 50 mA. The scanner can be operated in a 1 × 1 binning mode, where individual detectors are used at their highest native resolution. In 2 × 2 binning mode, four neighboring detectors are averaged to boost the signal-to-noise ratio at the expense of spatial resolution. The flat-panel volume CT scanner provides an effective field of view of 25 × 25 × 4.5 cm in the 1 × 1 binning mode and 25 × 25 × 18 cm in the 2 × 2 binning mode. The highest resolution achievable by using the system is 150 μm in the 1 × 1 binning mode and approximately 200 μm in the 2 × 2 binning mode. A modified Feldkamp algorithm is used for cone-beam reconstruction (26).

Flat-panel volume CT of the nondominant distal radius was performed in all subjects. None of the subjects had a history of fracture of the distal radius. During the examination, the wrist of the subject was immobilized in a foam cushion, and the subject was scanned in the standing position, with only the wrist positioned in the scanner. The hand was positioned by aligning it with the laser lights built into the scanner, such that the wrist joint was approximately aligned with the isocenter. The distal radius, including the growth plate, was scanned, and 100 CT sections were obtained and reformatted, starting 1 cm proximal to the most proximal portion of the articular surface of the distal radius, close to the distal radioulnar joint, delivering a three-dimensional representation of approximately 20 mm in the axial direction. The imaging was conducted at 100 kV and 30 mA, with a pulsed x-ray source in the 2 × 2 binning mode (voxel size, 0.2 × 0.2 × 0.2 mm^3). A 50% x-ray duty cycle was used. Scan time was 20 seconds. The radiation dose for a flat-panel volume CT scan of the distal radius was 0.027 mSv. Each subject was scanned with a calibration phantom to standardize gray-scale values and maintain consistency. A custom-designed calibration phantom consisting of three test tubes embedded in a foam cushion attached to a hand splint was used for stabilizing the wrist joint. The patient's hand was placed directly on the foam to ensure that the calibration tubes were as close to the distal radius as possible. The first test tube contained normal saline to provide calibration for 0 HU. The other two test tubes contained calibrated solutions of $Ca^2(HPO_4)^3$ that measured 130 and 200 HU with a conventional multidetector CT unit.

Measurement of Bone Microarchitecture

Trabecular structure parameters were calculated by using software (MicroView; GE Healthcare, Waukesha, Wis). For each distal radius, a three-dimensional oval region of interest was defined within the distal radius to cover a maximum area of trabecular bone with-

out including any cortical bone within the region of interest. Regions of interest were customized to the cross-sectional area for each scan. To improve reproducibility, all regions of interest were placed by one observer (M.A.B., with more than 10 years of musculoskeletal radiology experience). The observer was blinded to the patient status (AN vs control subject). Trabecular bone was then segmented from marrow, with the individual threshold level defined by the automatic threshold level function of the software. The automatic threshold level function provides automated segmentation by generating the attenuation histogram of the volume of interest and fitting the data by using the Otsu algorithm (30).

By using standard methods from histomorphometry (31), the following apparent measures of trabecular structure were calculated: apparent trabecular bone volume fraction (BV/TV) as a percentage, apparent trabecular number (TbN) in cubic millimeters, apparent trabecular thickness (TbTh) in millimeters, and apparent trabecular separation (TbSp) in millimeters. These parameters are defined as "apparent" because the spatial resolution is lower than that required for standard bone histomorphometry.

To establish stability of the measured structural bone parameters from one scan to the next (interscan variability), a set of five ex vivo cadaveric knee specimens was repeatedly scanned. To determine inter- and intraobserver variability, the structural parameters were measured in the proximal tibia by three readers (I.M., A.S., and A.C., each with 2 years of radiology experience) three times on 3 separate days. Interscan variability, which requires repeated scanning of the same anatomic structure, cannot be estimated in our adolescent population because of radiation concerns. To obtain inter- and intraobserver variability for the distal radius, structural parameters from 10 subjects were measured twice on 2 separate days by two readers (M.A.B. and A.C.).

DXA Assessment

We used DXA (QDR 4500; Hologic, Waltham, Mass) to measure BMD and body composition. The following parameters were obtained: BMD of the spine (L1–L4), BMD of the hip and femoral neck, total body BMD, total bone mineral content, bone mineral content adjusted for height, fat mass (in kilograms), lean mass (in kilograms), and percentage of body fat. The *z* scores were calculated for the spine, hip, and total body by using a normative age- and sex-based database for children supplied by the manufacturer of the scanner. This database is based on chronologic age. The *z* scores that were less than −2.0 were classified as "below expected range for age." BMD measurements of the distal radius were not performed because of the lack of normative data in children. Because DXA measures areal rather than volumetric bone density, it leads to an overestimate of bone density in tall children and an underestimate of bone density in short children. To correct for height, we used measures of bone mineral apparent density for the spine, calculated by using the formula described by Carter et al (6) and Katzman et al (32), and also obtained measures of whole-body bone mineral content divided by height. Coefficients of variation of DXA have been reported as less than 1% for bone (33), 4.1% for body fat mass, and 1.0% for lean body mass (34,35).

Table 1

Clinical Characteristics of AN and Control Groups

Variable	AN Group ($n = 10$)*	Control Group ($n = 10$)*	*P* Value
Chronologic age (y)	15.9 ± 1.6	15.9 ± 2.1	.96
Bone age (y)	15.9 ± 1.01	16.1 ± 2.1	.8
Age at menarche (y)	12.5 ± 1.3	12 ± 1.5	.45
BMI (kg/m^2)	18.4 ± 0.95	20.5 ± 2.6	.03†
Weight (kg)	50.9 ± 4.1	54.9 ± 10.6	.27
Height (cm)	165.8 ± 7.8	163 ± 7.7	.43
Tanner stage	4.8 ± 0.4	4.5 ± 0.7	.44
Duration of disease (mo)	13.8 ± 11.8	. . .	. . .
Fat mass (kg)	10.53 ± 1.6	14.74 ± 5.34	.02†
Lean mass (kg)	39.3 ± 4.15	39.1 ± 6.45	.91
Percentage of body fat	20.39 ± 3.14	25.89 ± 5.02	.009†

* Data are the mean ± SD.

† Significant difference.

Statistical Analysis

Statistical analysis was performed by using software (JMP; SAS Institute, Cary, NC). The means and SDs of structure parameters were calculated for the AN and control groups. Groups were compared by using the Student *t* test.

Linear regression analysis between trabecular structure parameters and BMD measurements at the different sites and between structure parameters and body composition parameters was performed. The slopes of the regression lines were compared between the groups to determine significant differences. Because this was a preliminary study with a small patient population, we did not adjust for multiple comparisons in the regression analysis model. It was more important to show the difference between the two groups rather than to show a significant nonzero correlation in each group.

The Bland-Altman analysis was used to assess interscan, interobserver, and intraobserver agreement for each trabecular structure parameter. Values are expressed as a percentage of the mean ± SD.

Results

Clinical Characteristics

Adolescent girls with AN did not differ from healthy control subjects in chro-

nologic age, bone age, or Tanner stage (Table 1). Adolescent girls with AN had lower BMI, fat mass, and percentage of body fat compared with control subjects, as expected, whereas there was no significant difference in lean mass between the two groups.

Interscan, Interobserver, and Intraobserver Variability

Interscan, interobserver, and intraobserver variability values for each trabecular structure parameter were low and are shown in Table 2.

Trabecular Structure

Flat-panel volume CT delineated trabecular structure of the distal radius in AN and control subjects (Fig 1). Trabecular structure measurements were significantly different between AN and control groups. Subjects with AN showed significantly lower values in BV/TV (0.37% ± 0.05 vs 0.46% ± 0.03, $P = .0002$) and TbTh (0.31 mm ± 0.03 vs 0.39 mm ± 0.03, $P < .0001$) and higher values in TbSp (0.54 mm ± 0.13 vs 0.44 mm ± 0.04, $P = .02$) compared with control subjects. TbN was lower in the AN group, but the difference was not significant (Table 3).

BMD Measurements

There was no significant difference in BMD measurements of the spine and hip between subjects with AN and control subjects (Table 4).

Relationship between Body Composition and Trabecular Structure Parameters

In the control group, there was a positive correlation between BMI and BV/TV ($r = 0.64$, $P = .04$), between BMI and TbTh ($r = 0.79$, $P = .006$), between fat mass and BV/TV ($r = 0.72$, $P = .01$), and between percentage of body fat and BV/TV ($r = 0.7$, $P = .02$) (Table E1 [*http://radiology.rsnajnls.org/cgi/content/full/249/3/938/DC1*]).

In the AN group, there was a positive correlation between fat mass and TbN ($r = 0.72$, $P = .01$) and between percentage of body fat and TbN ($r = 0.61$, $P = .05$). There was no significant correlation among BMI, fat mass, and percentage of body fat and the remaining trabecular structure parameters. There was no significant correlation between trabecular structure parameters and lean mass in the AN and control groups.

Table 2

Bland-Altman Analysis for Variability of Studies

Study and Variability	BV/TV	TbTh	TbN	TbSp
Knee study				
Interscan	0 ± 6.9	0 ± 2.9	0 ± 4.8	0 ± 8.4
Interobserver	1.5 ± 6.0	0.9 ± 3.1	1.2 ± 5.0	1.4 ± 8.5
Intraobserver	0.8 ± 6.0	0.9 ± 3.1	1.2 ± 5.0	1.4 ± 8.5
Distal radius study				
Interobserver	2.5 ± 6.1	0.3 ± 3.8	2.0 ± 4.2	4.0 ± 9.7
Intraobserver	0.1 ± 6.1	3.1 ± 4.6	0.6 ± 5.8	2.8 ± 8.6

Note.—Studies in the knee were ex vivo, and those in the distal radius were in vivo. Data are percentages of the mean ± SD.

Figure 1

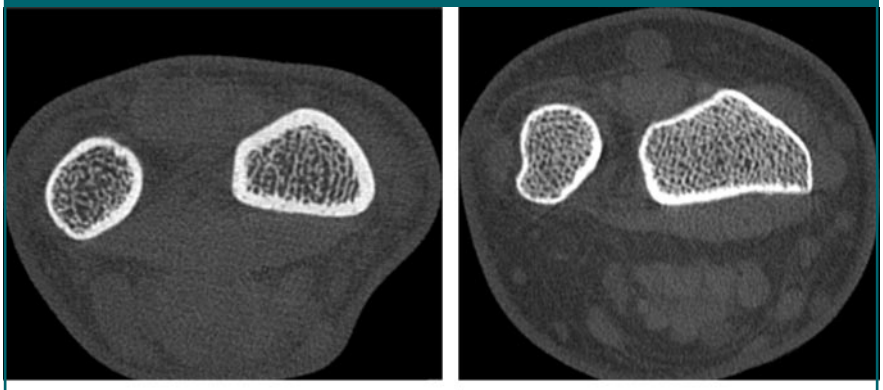

a. **b.**

Figure 1: **(a)** High-resolution flat-panel volume CT scan of distal radius in 15-year-old adolescent girl with AN (bone age, 16 years; BMI, 19.6 kg/m^2) demonstrates rarefaction of trabeculae of distal radius and ulna. Note lack of subcutaneous and deep fat. BV/TV was 0.25%; TbTh, 0.31 mm; TbN, 0.8/mm^{-3}; and TbSp, 0.9 mm. Total BMD was 1.156 g/cm^2; *z* score, 1.399. **(b)** High-resolution flat-panel volume CT scan of distal radius in 16-year-old normal-weight control subject (bone age, 17 years; BMI, 24.2 kg/m^2) demonstrates normal mineralization of distal radius and ulna. An increase was observed in trabeculae compared with trabeculae in AN subject in **a**. BV/TV was 0.54%; TbTh, 0.43 mm; TbN, 1.3/mm^{-3}; and TbSp, 0.37 mm. Total BMD was 1.106 g/cm^2; *z* score, 1.228.

Table 3

Trabecular Structure Parameters in AN and Control Groups

Variable	AN Group ($n = 10$)*	Control Group ($n = 10$)*	*P* Value
BV/TV (%)	0.37 ± 0.05	0.46 ± 0.03	.0002†
TbTh (mm)	0.31 ± 0.03	0.39 ± 0.03	<.0001†
TbN (mm^{-3})	1.17 ± 0.15	1.22 ± 0.07	.43
TbSp (mm)	0.54 ± 0.13	0.44 ± 0.04	.02†

* Data are the mean ± SD.

† Significant difference.

Relationship between BMD and Trabecular Structure Parameters

In the control group, there was a significant positive correlation between the trabecular structure parameters BV/TV

and TbTh with multiple BMD parameters. No significant correlation was observed between BV/TV or TbTh and hip BMD, hip *z* score, total BMD *z* score, and total bone mineral content divided by height. In addition, there was no significant correlation between TbN or TbSp and any of the BMD parameters. In the AN group, however, there was no significant correlation between any of the trabecular structure parameters and BMD parameters (Table E2 [*http://radiology.rsnajnls.org/cgi/content/full/249/3/938/DC1*]) Figure 2 shows regression analysis of AN and control groups for anteroposterior BMD lumbar spine and lateral lumbar spine BMD, with BV/TV and TbTh.

Discussion

Adolescence is the most critical period across the life span for the accrual of peak bone mass. The onset of AN during adolescence interferes with this process, and suboptimal peak bone mass will impair bone health later in life. Several studies have indicated that onset of AN in adolescence results in greater deficits in bone mass than disease onset during adulthood (36,37). However, bone mass measurements do not necessarily translate into fracture risk, which is better predicted by using measures of bone structure (10–16), and it is not known whether bone structural changes precede changes in bone density. Therefore, assessment of trabecular bone architecture is of particular concern during this period when the body is actively accruing bone mass. In this study, we compared bone structure parameters in adolescent girls with AN without extreme weight loss versus healthy age- and sex-matched normal-weight control subjects who did not differ with regard to BMD measures, as assessed by using DXA. We observed significant reductions in BV/TV and TbTh and increases in TbSp in the AN group. Our data indicate significant deleterious effects on bone micorarchitectural parameters in patients with AN even before changes in BMD are evident.

Most studies about patients with AN have used DXA to evaluate BMD. However, using DXA to measure BMD in children with AN has several limitations. Areal BMD leads to underestimates of BMD in short children and overestimates of BMD in tall children (6). This can be problematic in adolescents going through puberty at different times, because the timing of the growth spurt of puberty in these teenagers is variable. This is of particular importance in girls with AN in whom puberty is stalled or delayed and also because prolonged undernutrition can potentially lead to impaired statural growth.

Researchers in several studies have used CT and magnetic resonance imaging to assess and analyze trabecular structure in vivo (10,16,20,38–41). Use of the distal radius for structure analysis has proved valuable in the prediction of vertebral fractures (20). The trabecular bone content of the distal radius makes it a suitable choice for measurements of trabecular microstructure parameters with CT. The peripheral location of the distal radius allows a CT scan to be obtained quickly and easily. The distal radius also is relatively radioinsensitive, and no other organ receives direct or scattered radiation during scanning. These features allow a relatively low-dose CT scan to be obtained, a factor that is especially important in adolescents. We used the flat-panel volume CT prototype as a technique for evaluating trabecular structure. Flat-panel volume CT allows the examination of a volume of bone at high resolution (150–200 μm) with relatively low radiation exposure, making it a suitable technique for the evaluation of trabecular structure in adolescent patients. As demonstrated by our validation study, interscan, intraobserver, and interobserver variability parameters are low, thus making flat-panel volume CT a reliable technique for trabecular structure analysis.

Our results show that trabecular structure parameters of the distal radius, measured by using flat-panel volume CT, provide markers that can be used to differentiate between adolescents with AN and normal-weight control subjects. These markers are relatively easy to measure, have negligible radiation exposure as compared with background radiation, and show significant differences even in a setting of mild and early disease. The BMD measurements obtained by using DXA do not meet these criteria.

In our study, there was no signifi-

Table 4

BMD Parameters Measured with DXA in AN and Control Groups

Variable	AN Group ($n = 10$)*	Control Group ($n = 10$)*	*P* Value
Anteroposterior lumbar spine			
BMD (g/cm^2)	0.91 ± 0.08	0.9 ± 0.17	.8
BMD *z* score	−0.5 ± 0.99	−0.61 ± 1.13	.82
Bone mineral apparent density (g/cm^3)	0.14 ± 0.02	0.14 ± 0.03	.97
Bone mineral apparent density *z* score	−0.96 ± 0.95	−0.96 ± 1.19	.99
Lateral lumbar spine BMD (g/cm^2)	0.76 ± 0.07	0.77 ± 0.13	.89
Hip			
BMD (g/cm^2)	0.91 ± 0.08	0.88 ± 9.17	.61
z Score	−0.22 ± 0.64	−0.51 ± 1.32	.54
Femoral neck			
BMD (g/cm^2)	0.82 ± 0.08	0.79 ± 0.17	.56
z Score	−0.56 ± 0.74	−0.69 ± 1.31	.8
Whole body			
BMD (g/cm^2)	1.04 ± 0.05	1.0 ± 0.09	.48
BMD *z* score	0.09 ± 0.71	−0.32 ± 0.86	.25
Bone mineral content divided by height (g/cm)	11.9 ± 0.99	10.25 ± 3.91	.93
Bone mineral content divided by height *z* score	−0.3 ± 0.41	−0.2 ± 3.7	.93

* Data are the mean ± SD.

Figure 2

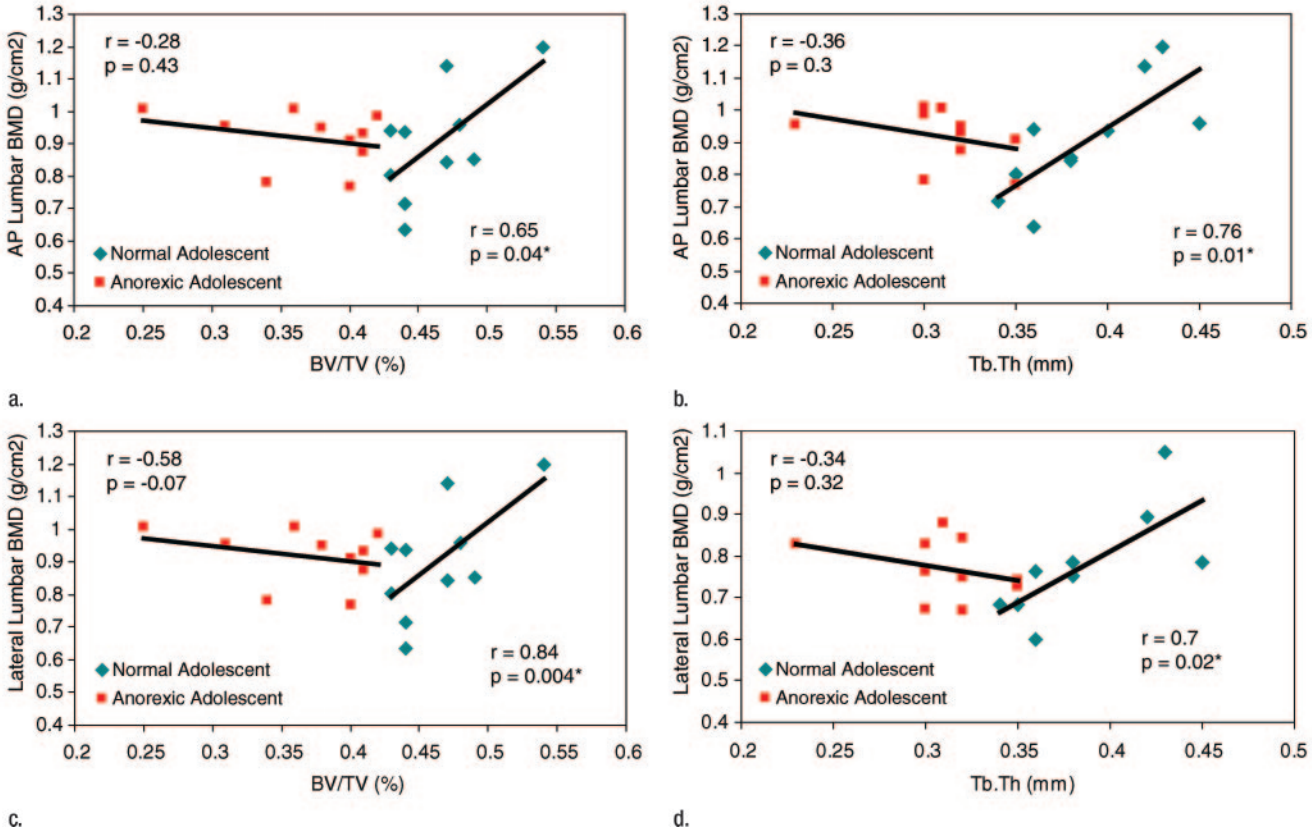

Figure 2: Regression analysis between lumbar spine BMD and trabecular structure parameters. Positive correlation was observed between **(a)** anteroposterior *(AP)* lumbar spine BMD and BV/TV, **(b)** anteroposterior lumbar spine BMD and TbTh, **(c)** lateral lumbar spine BMD and BV/TV, and **(d)** lateral lumbar spine and TbTh in normal-weight control subjects but not in AN patients. ∗ = significant.

cant difference in BMD between the AN and normal-weight control groups. Several studies in adolescents with AN have shown deceased BMD compared with normal-weight control subjects (5,21, 22,42). In these studies, patients with AN had more severe disease, as manifested by low BMI compared with our population (mean BMI, 15–16 vs 18 kg/m^2). This indicates that even in early or mild forms of AN, trabecular structure is already abnormal, whereas BMD remains within normal limits. These data are of great concern and suggest that reassuring values of BMD obtained by using DXA may not reflect the true status of bone structure in this undernourished population and that alterations in bone structure may occur well before significant decreases in BMD become evident, especially when dealing with early or mild disease.

In addition, the adolescent years are characterized by an increase in TbTh (43–45). The approximately 20% lower TbTh value in our subjects with AN compared with healthy control subjects (0.31 vs 0.39 mm, $P < .0001$) demonstrates an inability of the AN group to achieve pubertal norms for this parameter. This has potential consequences for bone strength in adult life.

Most of the studies on bone microstructure have been performed in adult patients with osteoporosis and compression fractures, and only a few studies have been performed in AN patients with analysis of bone microstructure (21–23). Milos et al (22) found significant differences in BV/TV, TbN, and TbSp but not TbTh in adults with AN compared with normal-weight control subjects. The lower TbTh in our adolescent population, as opposed to no change in TbTh in adults with AN, probably reflects an impairment of the normal increase in TbTh that is characteristic of the pubertal years. Galusca et al (21) showed differences in structure parameters of the distal radius and tibia in adult patients with AN, as compared with normal-weight control subjects, only when there was a long-standing history of AN. Our study focused on adolescents with AN with relatively mild disease and a short duration of disease.

In our study, none of the BMD parameters showed significant correlation in the AN group, whereas there was a positive correlation between trabecular structure parameters, especially BV/TV and TbTh with several BMD parameters in the control group. This suggests that BMD adequately measures bone health in the healthy control population, but this association breaks down as a statis-

tically valid parameter in AN patients, even when the disease is mild. Our data also indicate that the alterations of trabecular microarchitecture in patients with AN follow an unpredictable course.

Our study had several limitations. First, this was a relatively small group of subjects. However, even with 10 subjects in each group, we were able to see a significant difference in structure parameters between AN adolescents and normal-weight control subjects. Second, our study design was cross sectional, and the lack of follow-up did not allow evaluation of true fracture risk. Larger longitudinal studies are necessary to confirm that alterations in trabecular structure parameters in adolescents with AN lead to an increased risk of fractures in this population. However, investigators in several studies have demonstrated that trabecular bone structure in patients with osteoporosis can be used to strongly predict fracture risk (14,16). It can, therefore, be inferred that similar alterations in the trabecular structure induced by AN would lead to similarly increased fracture risk. Third, our data about interscan variability were obtained at a different site (proximal tibia) and not at the distal radius. Fourth, the trabecular diameter ranges normally from 100–200 μm, and the spatial resolution of flat-panel volume CT is insufficient to resolve smaller trabeculae.

In conclusion, flat-panel volume CT is a useful technique for the evaluation of trabecular structure in patients with AN, even in the setting of mild or early disease. Even with mild disease, the bone structure is abnormal in adolescents with AN compared with normal-weight control subjects despite normal BMD. Given the increasing prevalence of AN and its profound consequences on bone health, these results may have major implications in the treatment and follow-up of patients with AN. It will be important to determine whether therapies that increase BMD will concomitantly improve bone structure in this patient population.

Acknowledgments: We thank Christianne Leidecker, PhD, and Michael Grasruck, PhD, of Siemens Medical Solutions, Forchheim, Germany, for their technical help with the flat-panel volume CT scanner. We also thank Jennalee Cord, BA, and Nara Mendes, BA, for their help in patient recruitment and study coordination.

References

1. Grinspoon S, Thomas E, Pitts S, et al. Prevalence and predictive factors for regional osteopenia in women with anorexia nervosa. Ann Intern Med 2000;133:790–794.
2. Misra M, Aggarwal A, Miller KK, et al. Effects of anorexia nervosa on clinical, hematologic, biochemical, and bone density parameters in community-dwelling adolescent girls. Pediatrics 2004;114:1574–1583.
3. Vestergaard P, Emborg C, Stoving RK, Hagen C, Mosekilde L, Brixen K. Fractures in patients with anorexia nervosa, bulimia nervosa, and other eating disorders: a nationwide register study. Int J Eat Disord 2002;32:301–308.
4. Misra M, Klibanski A. Anorexia nervosa and osteoporosis. Rev Endocr Metab Disord 2006;7:91–99.
5. Misra M, Prabhakaran R, Miller KK, et al. Prognostic indicators of changes in bone density measures in adolescent girls with anorexia nervosa. II. J Clin Endocrinol Metab 2008;93:1292–1297.
6. Carter DR, Bouxsein ML, Marcus R. New approaches for interpreting projected bone densitometry data. J Bone Miner Res 1992; 7:137–145.
7. DiVasta AD, Ringelheim J, Bristol SK, Feldman HA, Gordon CM. Skeletal measurements by quantitative ultrasound in adolescents and young women with anorexia nervosa. J Pediatr 2007; 150:286–290, 290.e1.
8. Resch H, Newrkla S, Grampp S, et al. Ultrasound and x-ray-based bone densitometry in patients with anorexia nervosa. Calcif Tissue Int 2000;66:338–341.
9. Guglielmi G, Lang TF. Quantitative computed tomography. Semin Musculoskelet Radiol 2002;6:219–227.
10. Kleerekoper M, Villanueva AR, Stanciu J, Rao DS, Parfitt AM. The role of three-dimensional trabecular microstructure in the pathogenesis of vertebral compression fractures. Calcif Tissue Int 1985;37:594–597.
11. Ross PD, Wasnich RD, Davis JW. Fracture prediction models for osteoporosis prevention. Bone 1990;11:327–331.
12. Ross PD, Davis JW, Vogel JM, Wasnich RD. A critical review of bone mass and the risk of fractures in osteoporosis. Calcif Tissue Int 1990;46:149–161.
13. Link TM, Vieth V, Matheis J, et al. Bone structure of the distal radius and the calcaneus vs BMD of the spine and proximal femur in the prediction of osteoporotic spine fractures. Eur Radiol 2002;12:401–408.
14. Patel PV, Prevrhal S, Bauer JS, et al. Trabecular bone structure obtained from multislice spiral computed tomography of the calcaneus predicts osteoporotic vertebral deformities. J Comput Assist Tomogr 2005;29: 246–253.
15. Wehrli FW, Song HK, Saha PK, Wright AC. Quantitative MRI for the assessment of bone structure and function. NMR Biomed 2006; 19:731–764.
16. Boutroy S, Bouxsein ML, Munoz F, Delmas PD. In vivo assessment of trabecular bone microarchitecture by high-resolution peripheral quantitative computed tomography. J Clin Endocrinol Metab 2005;90:6508–6515.
17. Chen P, Miller PD, Recker R, et al. Increases in BMD correlate with improvements in bone microarchitecture with teriparatide treatment in postmenopausal women with osteoporosis. J Bone Miner Res 2007;22: 1173–1180.
18. Benhamou CL. Effects of osteoporosis medications on bone quality. Joint Bone Spine 2007;74:39–47.
19. Cummings SR, Nevitt MC, Browner WS, et al. Risk factors for hip fracture in white women: study of Osteoporotic Fractures Research Group. N Engl J Med 1995;332:767–773.
20. Link TM, Bauer J, Kollstedt A, et al. Trabecular bone structure of the distal radius, the calcaneus, and the spine: which site predicts fracture status of the spine best? Invest Radiol 2004;39:487–497.
21. Galusca B, Zouch M, Germain N, et al. Constitutional thinness: unusual human phenotype of low bone quality. J Clin Endocrinol Metab 2008;93:110–117.
22. Milos G, Spindler A, Ruegsegger P, et al. Cortical and trabecular bone density and structure in anorexia nervosa. Osteoporos Int 2005;16:783–790.
23. Milos G, Spindler A, Ruegsegger P, et al. Does weight gain induce cortical and trabecular bone regain in anorexia nervosa? a 2-year prospective study. Bone 2007;41: 869–874.
24. Bartling SH, Shukla V, Becker H, Brady TJ, Hayman A, Gupta R. High-resolution flat-panel volume-CT of temporal bone. I. Axial preoperative anatomy. J Comput Assist Tomogr 2005;29:420–423.
25. Gupta R, Bartling SH, Basu SK, et al. Exper-

imental flat-panel high-spatial-resolution volume CT of the temporal bone. AJNR Am J Neuroradiol 2004;25:1417–1424.

26. Gupta R, Grasruck M, Suess C, et al. Ultra-high resolution flat-panel volume CT: fundamental principles, design architecture, and system characterization. Eur Radiol 2006; 16:1191–1205.

27. Buie HR, Campbell GM, Klinck RJ, MacNeil JA, Boyd SK. Automatic segmentation of cortical and trabecular compartments based on a dual threshold technique for in vivo micro-CT bone analysis. Bone 2007;41:505–515.

28. Kalender WA. The use of flat-panel detectors for CT imaging [in German]. Radiologe 2003;43:379–387.

29. Greulich WW, Pyle SI. Radiographic atlas of skeletal development of the hand and wrist. 2nd ed. Stanford, Calif: Stanford University Press, 1959.

30. Otsu N. A threshold selection method from gray-level histograms. IEEE Trans Syst Man Cybern 1979;9:62–66.

31. Parfitt AM. Bone histomorphometry: proposed system for standardization of nomenclature, symbols, and units. Calcif Tissue Int 1988;42:284–286.

32. Katzman DK, Bachrach LK, Carter DR, Marcus R. Clinical and anthropometric correlates of bone mineral acquisition in healthy adolescent girls. J Clin Endocrinol Metab 1991;73:1332–1339.

33. Barthe N, Braillon P, Ducassou D, Basse-Cathalinat B. Comparison of two Hologic DXA systems (QDR 1000 and QDR 4500/A). Br J Radiol 1997;70:728–739.

34. Pintauro SJ, Nagy TR, Duthie CM, Goran MI. Cross-calibration of fat and lean measurements by dual-energy x-ray absorptiometry to pig carcass analysis in the pediatric body weight range. Am J Clin Nutr 1996;63: 293–298.

35. van der Sluis IM, de Ridder MA, Boot AM, Krenning EP, de Muinck Keizer-Schrama SM. Reference data for bone density and body composition measured with dual energy x ray absorptiometry in white children and young adults. Arch Dis Child 2002;87: 341–347.

36. Biller BM, Saxe V, Herzog DB, Rosenthal DI, Holzman S, Klibanski A. Mechanisms of osteoporosis in adult and adolescent women with anorexia nervosa. J Clin Endocrinol Metab 1989;68:548–554.

37. Seeman E, Karlsson MK, Duan Y. On exposure to anorexia nervosa, the temporal variation in axial and appendicular skeletal development predisposes to site-specific deficits in bone size and density: a cross-sectional study. J Bone Miner Res 2000;15:2259–2265.

38. Ladinsky GA, Wehrli FW. Noninvasive assessment of bone microarchitecture by MRI. Curr Osteoporos Rep 2006;4:140–147.

39. Link TM, Majumdar S. Current diagnostic techniques in the evaluation of bone architecture. Curr Osteoporos Rep 2004;2: 47–52.

40. Link TM, Majumdar S, Grampp S, et al. Imaging of trabecular bone structure in osteoporosis. Eur Radiol 1999;9:1781–1788.

41. Phan CM, Matsuura M, Bauer JS, et al. Trabecular bone structure of the calcaneus: comparison of MR imaging at 3.0 and 1.5 T with micro-CT as the standard of reference. Radiology 2006;239:488–496.

42. Misra M, Miller KK, Cord J, et al. Relationships between serum adipokines, insulin levels, and bone density in girls with anorexia nervosa. J Clin Endocrinol Metab 2007;92: 2046–2052.

43. Byers S, Moore AJ, Byard RW, Fazzalari NL. Quantitative histomorphometric analysis of the human growth plate from birth to adolescence. Bone 2000;27:495–501.

44. Parfitt AM, Travers R, Rauch F, Glorieux FH. Structural and cellular changes during bone growth in healthy children. Bone 2000; 27:487–494.

45. Rauch F. Bone accrual in children: adding substance to surfaces. Pediatrics 2007; 119(suppl 2):S137–S140.

Radiology 2008

This is your reprint order form or pro forma invoice

(Please keep a copy of this document for your records.)

Reprint order forms and purchase orders or prepayments must be received 72 hours after receipt of form either by mail or by fax at 410-820-9765. It is the policy of Cadmus Reprints to issue one invoice per order. **Please print clearly**.

Author Name _____
Title of Article _____
Issue of Journal_____ Reprint # _____ Publication Date _____
Number of Pages_____ KB # _____ Symbol Radiology
Color in Article? Yes / No (Please Circle)

Please include the journal name and reprint number or manuscript number on your purchase order or other correspondence.

Order and Shipping Information

Reprint Costs **(Please see page 2 of 2 for reprint costs/fees.)**

_____ Number of reprints ordered $_____
_____ Number of color reprints ordered $_____
_____ Number of covers ordered $_____
Subtotal $_____
Taxes $_____

(*Add appropriate sales tax for Virginia, Maryland, Pennsylvania, and the District of Columbia or Canadian GST to the reprints if your order is to be shipped to these locations*.)

First address included, add $32 for each additional shipping address $_____

TOTAL $_____

Shipping Address **(cannot ship to a P.O. Box) Please Print Clearly**

Name _____
Institution _____
Street _____
City _____ State _____ Zip _____
Country _____
Quantity_____ Fax _____
Phone: Day _____ Evening _____
E-mail Address _____

Additional Shipping Address* **(cannot ship to a P.O. Box)**

Name _____
Institution _____
Street _____
City _____ State _____ Zip _____
Country _____
Quantity _____ Fax _____
Phone: Day _____ Evening _____
E-mail Address _____
** Add $32 for each additional shipping address*

Payment and Credit Card Details

Enclosed: Personal Check _____
Credit Card Payment Details _____
Checks must be paid in U.S. dollars and drawn on a U.S. Bank.

Credit Card: __ VISA __ Am. Exp. __ MasterCard
Card Number _____
Expiration Date_____
Signature: _____

Please send your order form and prepayment made payable to:

Cadmus Reprints
P.O. Box 751903
Charlotte, NC 28275-1903

Note: Do not send express packages to this location, PO Box.
FEIN #:541274108

Invoice or Credit Card Information

Invoice Address Please Print Clearly
Please complete Invoice address as it appears on credit card statement

Name _____
Institution _____
Department _____
Street _____
City _____ State _____ Zip _____
Country _____
Phone _____ Fax _____
E-mail Address _____

Cadmus will process credit cards and *Cadmus Journal Services* will appear on the credit card statement.

If you don't mail your order form, you may fax it to 410-820-9765 with your credit card information.

Signature _____ Date _____
Signature is required. By signing this form, the author agrees to accept the responsibility for the payment of reprints and/or all charges described in this document.

RB-9/26/07

Radiology 2008

Black and White Reprint Prices

Domestic (USA only)						
# of Pages	50	100	200	300	400	500
1-4	$221	$233	$268	$285	$303	$323
5-8	$355	$382	$432	$466	$510	$544
9-12	$466	$513	$595	$652	$714	$775
13-16	$576	$640	$749	$830	$912	$995
17-20	$694	$775	$906	$1,017	$1,117	$1,220
21-24	$809	$906	$1,071	$1,200	$1,321	$1,471
25-28	$928	$1,041	$1,242	$1,390	$1,544	$1,688
29-32	$1,042	$1,178	$1,403	$1,568	$1,751	$1,924
Covers	$97	$118	$215	$323	$442	$555

International (includes Canada and Mexico)						
# of Pages	50	100	200	300	400	500
1-4	$272	$283	$340	$397	$446	$506
5-8	$428	$455	$576	$675	$784	$884
9-12	$580	$626	$805	$964	$1,115	$1,278
13-16	$724	$786	$1,023	$1,232	$1,445	$1,652
17-20	$878	$958	$1,246	$1,520	$1,774	$2,030
21-24	$1,022	$1,119	$1,474	$1,795	$2,108	$2,426
25-28	$1,176	$1,291	$1,700	$2,070	$2,450	$2,813
29-32	$1,316	$1,452	$1,936	$2,355	$2,784	$3,209
Covers	$156	$176	$335	$525	$716	$905

Color Reprint Prices

Domestic (USA only)						
# of Pages	50	100	200	300	400	500
1-4	$223	$239	$352	$473	$597	$719
5-8	$349	$401	$601	$849	$1,099	$1,349
9-12	$486	$517	$852	$1,232	$1,609	$1,992
13-16	$615	$651	$1,105	$1,609	$2,117	$2,624
17-20	$759	$787	$1,357	$1,997	$2,626	$3,260
21-24	$897	$924	$1,611	$2,376	$3,135	$3,905
25-28	$1,033	$1,071	$1,873	$2,757	$3,650	$4,536
29-32	$1,175	$1,208	$2,122	$3,138	$4,162	$5,180
Covers	$97	$118	$215	$323	$442	$555

International (includes Canada and Mexico))						
# of Pages	50	100	200	300	400	500
1-4	$278	$290	$424	$586	$741	$904
5-8	$429	$472	$746	$1,058	$1,374	$1,690
9-12	$604	$629	$1,061	$1,545	$2,011	$2,494
13-16	$766	$797	$1,378	$2,013	$2,647	$3,280
17-20	$945	$972	$1,698	$2,499	$3,282	$4,069
21-24	$1,110	$1,139	$2,015	$2,970	$3,921	$4,873
25-28	$1,290	$1,321	$2,333	$3,437	$4,556	$5,661
29-32	$1,455	$1,482	$2,652	$3,924	$5,193	$6,462
Covers	$156	$176	$335	$525	$716	$905

Minimum order is 50 copies. For orders larger than 500 copies, please consult Cadmus Reprints at 800-407-9190.

Reprint Cover

Cover prices are listed above. The cover will include the publication title, article title, and author name in black.

Shipping

Shipping costs are included in the reprint prices. Domestic orders are shipped via UPS Ground service. Foreign orders are shipped via a proof of delivery air service.

Multiple Shipments

Orders can be shipped to more than one location. Please be aware that it will cost $32 for each additional location.

Delivery

Your order will be shipped within 2 weeks of the journal print date. Allow extra time for delivery.

Tax Due

Residents of Virginia, Maryland, Pennsylvania, and the District of Columbia are required to add the appropriate sales tax to each reprint order. For orders shipped to Canada, please add 7% Canadian GST unless exemption is claimed.

Ordering

Reprint order forms and purchase order or prepayment is required to process your order. Please reference journal name and reprint number or manuscript number on any correspondence. You may use the reverse side of this form as a proforma invoice. Please return your order form and prepayment to:

Cadmus Reprints
P.O. Box 751903
Charlotte, NC 28275-1903

Note: Do not send express packages to this location, PO Box.
FEIN #:541274108

Please direct all inquiries to:

Rose A. Baynard
800-407-9190 (toll free number)
410-819-3966 (direct number)
410-820-9765 (FAX number)
baynardr@cadmus.com (e-mail)

Reprint Order Forms and purchase order or prepayments must be received 72 hours after receipt of form.